

# Hole-hole and electron-hole exchange interactions in single InAs/GaAs quantum dots

T. Warming,<sup>1</sup> E. Siebert,<sup>1</sup> A. Schliwa,<sup>1</sup> E. Stock,<sup>1</sup> R. Zimmermann,<sup>2</sup> and D. Bimberg<sup>1</sup>

<sup>1</sup>*Institut für Festkörperphysik, Technische Universität Berlin, Hardenbergstrasse 36, 10623 Berlin, Germany*

<sup>2</sup>*Institut für Physik der Humboldt-Universität Berlin, Newtonstrasse 15, 12489 Berlin, Germany*

(Received 5 December 2008; revised manuscript received 26 January 2009; published 17 March 2009)

A combined analysis of microphotoluminescence ( $\mu$ PL) and microphotoluminescence excitation ( $\mu$ PLe) spectra of the same single quantum dot (QD) enables an unambiguous identification of four sharp resonances in the excitation spectrum detected on the positive trion transition ( $h_0 \rightarrow e_0 h_0 h_1$ ) and reveals the complete fine structure of the hot trion. Transitions into states normally forbidden by (spin) selection rules for optical transitions between pure spin states are observed. The splittings of all triplet states are found to be large (up to 3 meV), asymmetric, and QD size and shape dependent. The experimental data are in excellent agreement with theoretical calculations in the framework of eight-band  $\mathbf{k} \cdot \mathbf{p}$  theory and the configuration-interaction method. To account for the physical effects which lead to the observed fine-structure splitting, parts of the complex model are successively omitted. This approach identifies the anisotropic hole-hole exchange interaction as well as correlation effects dominating the observed fine-structure splitting of the hot trion.

DOI: [10.1103/PhysRevB.79.125316](https://doi.org/10.1103/PhysRevB.79.125316)

PACS number(s): 71.70.Gm, 73.21.La, 78.67.Hc

## I. INTRODUCTION

Single quantum dots (QDs) are the most promising candidates for future electrically driven emitters of qubits (single polarized photons) or entangled photon pairs.<sup>1–5</sup> Such emitters (together with highly efficient single-photon detectors) present the physical backbone of future quantum cryptography and communication systems. Exchange interaction of the electron and the hole populating the ground state of a QD leads to a fine-structure splitting (FSS). Size and sign of the fine-structure splitting depend on the size and shape of the QDs and control the properties of the emitted photons.<sup>6</sup> A detailed understanding of exchange interaction in these nanostructures is therefore of fundamental physical interest and utmost importance for system applications.

Symmetry-based arguments lead to a separation of the exchange interaction into an isotropic and an anisotropic part. The latter causes the splitting of the exciton bright states. The dark-bright splitting and the splitting of the exciton dark states are determined by the isotropic part of the electron-hole interaction.<sup>7–9</sup> As the dark states of the exciton are optically not accessible in the absence of an external magnetic field, its complete fine structure and therewith the exchange interaction cannot be probed spectroscopically.

The isotropic part of the exchange interaction is revealed however in the spectra of double charged excitons<sup>10,11</sup> and excited trions.<sup>12,13</sup> Their previous investigations by us and others were based on single-QD photoluminescence ( $\mu$ PL) or cathodoluminescence (CL). The observed ground-state transitions reflect only parts of the fine structure. Excited states, e.g., of the exciton or the trion, are hardly accessible by luminescence.

This drawback can be overcome by resonant excitation of single QDs using the excitation energy as a variable. Excited exciton states or, if the QD is charged, excited trions can be thus created. Photoluminescence excitation spectroscopy (PLE) has been successfully applied to QD ensembles<sup>14</sup> but only rarely for investigations of single InAs/GaAs QDs.<sup>15–18</sup>

Using  $\mu$ PLe not only bound-to-bound transitions are probed but also bound-to-continuum and continuum-to-

continuum transitions.<sup>17,19</sup> Additional resonances in PLe are caused by simultaneous generation of optical phonons.<sup>15</sup> One of the main difficulties of using  $\mu$ PLe to probe single QDs is the unambiguous assignment of the resonances in the spectrum to specific transitions.

This work presents twofold fundamental progress. Based on comparison of  $\mu$ PL and  $\mu$ PLe, the identification of the *complete* fine structure of the hot trion becomes possible. Calculations reveal anisotropic hole-hole exchange and correlation effects as the driving parameters for the fine-structure splitting of the hot trion. Experiment and theory are found to be in excellent agreement.

## II. ELECTRONIC STRUCTURE OF THE HOT TRION

A positively charged trion ( $X^+$ ) consists of one electron and two holes. All particles may occupy the ground state of the QD ( $e_0 h_0 h_0$ ) or at least one hole may occupy the first or higher excited state (e.g.,  $e_0 h_0 h_1$ , denoted  $X^{+*}$ ). The energetics of the latter, called *hot trion*, is the main subject of this paper for reasons discussed now. Since the various energy levels of the QD are occupied here by one particle only, the spins of the particles are independent, allowing  $2^3$  different spin configurations. The total spin of a hot trion has a half-integer value. According to Kramer's theorem all states have to be at least twofold degenerate in the absence of a magnetic field. Thus only four doubly-degenerate energy levels can arise. Their splitting is controlled by the exchange interaction (electron-hole,  $K_{eh}$ , and hole-hole,  $K_{hh}$ ) and correlation effects. If the excited hole occupies the first hole level the four hot trion levels are denoted by  $X_{1,\dots,4}^{+*}$ .

K. V. Kavokin<sup>20</sup> presented a theoretical analysis of such a trion, neglecting contributions of the light holes and intermixing of the singlet and triplet states. The system was simplified by a separation of the exchange interaction into terms of different sizes. The isotropic exchange interaction between identical particles, here between the two holes, is known to influence the electronic structure most. It splits the twofold-degenerate singlet  $S_{\pm 1/2}$  from the sixfold-degenerate

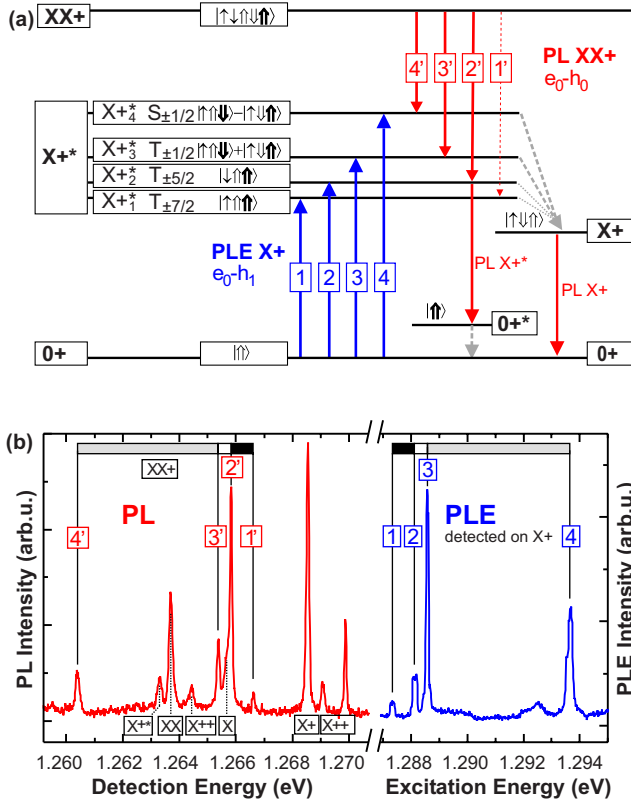


FIG. 1. (Color online) (a) Term scheme of a QD occupied with one hole, showing the correspondence between PLE (peaks 1, 2, 3, and 4) transitions and the PL of the charged biexciton (peaks 1', 2', 3', and 4'). All states are twofold degenerate. One possible spin configuration is indicated. ↑: electron; ↓: hole; bold marks occupation in the first-excited state. (b) Typical PL spectrum (left) and the related PLE spectrum detected at X+ (right). The correspondence between PLE lines and the XX+ PL enables the identification of the PLE lines. Identical energy separations are marked by bars of the same gray level in both spectra.

triplet states. The splitting of the triplet states is handled separately. The isotropic part of the electron-hole exchange leads to an equally spaced energy splitting of the three triplet states  $T_{\pm 7/2}$ ,  $T_{\pm 5/2}$ , and  $T_{\pm 1/2}$ . The anisotropic part of the electron-hole exchange interaction leads to mixing of these states. Further lifting of their degeneracy is prohibited by Kramer's theorem, resulting in four degenerate doublets as shown in Fig. 1(a). The interpretation of polarization effects in charged CdSe (Ref. 13) and InAs (Refs. 11, 12, and 18) QDs are based on this approach, which enables the assignment of spin configurations to the  $X_{1,\dots,4}^+$  states.

### III. EXPERIMENTAL RESULTS

The samples investigated in this paper were grown by molecular-beam epitaxy (MBE) on GaAs(001) substrates using growth conditions to get defect-free QDs. A buffer layer of 500 nm GaAs was grown at 585 °C. For the QD layer the temperature was reduced to 485 °C and nominally 2.5 monolayers of InAs were deposited and covered by 7 nm of GaAs before the temperature was raised to 585 °C again for

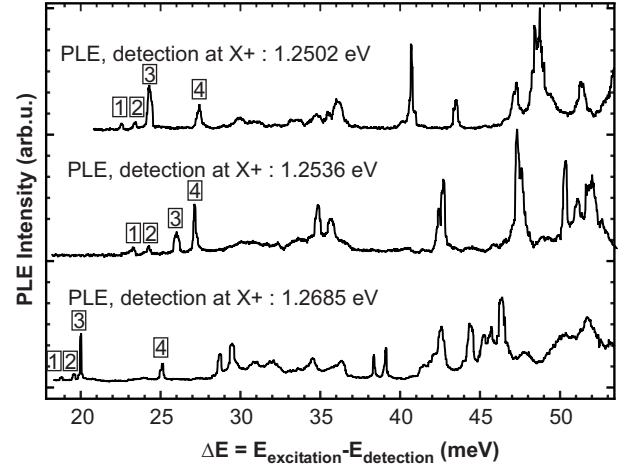


FIG. 2. PLE spectra of three different QDs detected on the transition energy of the positive trion. All spectra show at low excitation energy a group of four transitions to the four states of the hot trion ( $e_0^1 h_0^1 h_1^1$ ).

the growth of a 43 nm capping layer. The QD density is of the order of  $5 \times 10^{10} \text{ cm}^{-2}$  with the PL maximum at 1.119 eV [full width at half maximum (FWHM) 75 meV] at 15 K. For the single-dot measurements in this work, we choose QDs with exciton ground states between 1.23 and 1.27 eV on the high-energy side of this distribution. The dominance of positively charged complexes in  $\mu$ PL spectra indicates an unintentional positive background doping.

The PL was detected through a metal shadow mask with 100 and 200 nm apertures using a tunable cw Ti:sapphire laser as excitation source and a triple 0.5 m monochromator with a liquid N<sub>2</sub> cooled Si charge coupled device (CCD) for detection. All spectra were recorded at 15 K.

Single-QD  $\mu$ PL spectra [Fig. 1(b)] display the decay of different few-particle complexes due to a statistical occupation of the QD. Polarization and excitation density dependent measurements enable the assignment of most of the luminescence lines to specific few-particle complexes.<sup>21</sup>

The fine structure of the hot trion is partially revealed by the PL of the charged biexciton (XX+). The two emission lines corresponding to the decay to the  $X_{2,3}^+$  and  $X_{4,1}^+$  states are easily identified by their constant intensity ratio.<sup>12</sup> So far the decay to the  $X_{4,1}^+$  state, which corresponds to the singlet state  $S_{\pm 1/2}$  if intermixing of the states is negligible, has not been identified or observed in PL before.<sup>12,13</sup> The decay to the  $X_{1,2}^+$  state has also never been reported and is not expected to be observable in PL. Neglecting again intermixing of the  $X^+$  states,  $X_{1,2}^+$  corresponds to the triplet state  $T_{\pm 7/2}$ . The optical transition between XX+ and the  $T_{\pm 7/2}$  state of the  $X^+$  is forbidden by spin-selection rules.

The fingerprint of the complete fine-structure splitting of  $X_{1,2}^+$  is present in the  $\mu$ PLE spectra detected on X+. Figure 2 shows  $\mu$ PLE spectra of three different QDs. The  $\mu$ PLE spectra of all QDs show a group of four sharp resonances at low excitation energies (labeled as 1–4 in Fig. 2). Sharp resonances are observed only below  $\Delta E = 55$  meV, where  $\Delta E$  is the difference between excitation and detection energy. Above this energy a broad background, attributed to bound-to-continuum transitions,<sup>19</sup> is visible. The next challenge is

now the identification of the transitions corresponding to the hot trion states. For this purpose we compare for the same dot the energy separations of the  $XX+$  lines in  $\mu$ PL with those of the  $X+$  in  $\mu$ PLE.

A detailed  $\mu$ PLE of one QD, containing the transitions 1–4 from Fig. 2, is shown in Fig. 1(b) on the right-hand side. On the left-hand side the corresponding  $\mu$ PL of the same QD is plotted. The energy-level diagram [Fig. 1(a)] illustrates the relation between the energy separations in  $\mu$ PLE and  $\mu$ PL. In  $\mu$ PL the identification of the transitions from  $XX+$  to  $X+^*_2$  and  $X+^*_3$  states is well established.<sup>12</sup> They are labeled as 2' and 3' in Fig. 1. Identical splitting is now found in the  $\mu$ PLE spectra between the lines labeled as 2 and 3, permitting the unambiguous identification of the  $\mu$ PLE lines: a direct generation of  $X+^*$  by  $(e_0-h_1)$  generation. Theory<sup>22,23</sup> predicts zero oscillator strength for the  $e_0-h_1$  transitions for all QDs with a symmetry of  $C_{2v}$  or higher. Their observation indicates that the symmetry of the probed QDs is lower.

Having identified the resonances 2 and 3, the energy-level diagram [Fig. 1(a)] suggests the assignment of resonances 1 and 4 to the generation of the  $X+^*_1$  and  $X+^*_4$  states. The positive proof is found in  $\mu$ PL by comparing the energy separation of the hot trion states from  $\mu$ PLE to the  $\mu$ PL of  $XX+$ . Two additional yet unidentified peaks in the PL (1' and 4') can be assigned to the decay of  $XX+$  to hot trion states. The transition to the  $X+^*_4$  state (the singlet  $S_{\pm 1/2}$  state) is visible for all examined QDs; the decay to the  $X+^*_1$  state is observed only occasionally.

The combination of  $\mu$ PL and  $\mu$ PLE therefore allows a systematic analysis of the complete fine structure of the  $X+^*$ . The fine structure of a large number of QDs has been analyzed in this way. The energy of the exciton ground-state transition vary from 1.228 to 1.266 eV and is uncorrelated with the fine-structure splitting. In Fig. 3 the energetic position of the hot trion  $X+^*_{1,\dots,4}$  states relative to the energy of the  $X+^*_2$  state is plotted against the energy separation between  $X+^*_3$  and  $X+^*_2$ . Therewith correlations between variations in the different energy separations become transparent. Each QD is represented by four points which are vertically aligned, representing the four hot trion states. The  $\mu$ PLE data (full circles) are complemented by data from  $\mu$ PL (open squares) of additional QDs from the same sample, only including the  $X+^*_{2,3,4}$  states. The energy separation between  $X+^*_4$  and  $X+^*_2$  varies between 5.6 and 2.8 meV. The separation between  $X+^*_3$  and  $X+^*_2$  varies between 0.23 and 2.1 meV. The separation between the  $X+^*_1$  and  $X+^*_2$  states is between 0.81 and 0.95 meV.

The energy splittings are obviously anticorrelated. Whenever  $E(X+^*_4)-E(X+^*_2)$  is large,  $E(X+^*_3)-E(X+^*_2)$  is small. This indicates that a common parameter governs both splittings. If we consider the center of the  $X+^*_3$  and  $X+^*_4$  transitions  $[E(X+^*_4)-E(X+^*_3)]/2$ , the energy separation to the  $X+^*_2$  state is almost constant ( $\approx 2.7$  meV), indicating mixing between the  $X+^*_3$  and  $X+^*_4$  states as driving parameter. The variation in  $E(X+^*_1)-E(X+^*_2)$  is small but increases monotonically with increasing  $E(X+^*_3)-E(X+^*_2)$ . These experimental findings are in contrast to previous theoretical predictions<sup>20</sup> of a symmetric triplet splitting, which is only weakly affected by intermixing effects due to anisotropic electron-hole exchange interaction.

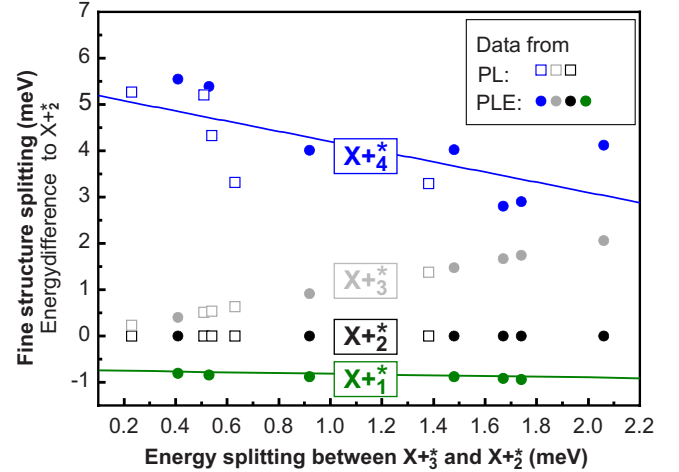


FIG. 3. (Color online) Fine structure of the hot trion of a number of QDs. The energetic position, relative to the energy of the  $X+^*_2$  state, is plotted against the energy splitting between  $X+^*_3$  and  $X+^*_2$  states. Each QD is represented by four points (PL data only three) which are aligned vertically. The  $X+^*_4-X+^*_2$  splitting and the  $X+^*_3-X+^*_2$  splitting show a clear anticorrelation with a slope of  $-1.1$  for the linear fit. The variation in  $E(X+^*_1)-E(X+^*_2)$  is small but increases monotonically with increasing  $E(X+^*_3)-E(X+^*_2)$  with a slope of  $0.075$ .

#### IV. THEORETICAL RESULTS

The electronic structure of the QDs is calculated using a three-dimensional implementation of the eight-band  $\mathbf{k}\cdot\mathbf{p}$  method. The model accounts for the inhomogeneous strain distribution, the built-in piezoelectric potential (including first-order<sup>24</sup> and second-order<sup>22,25,26</sup> effects), and interband mixing. Few-particle states (here the hot trion states) are calculated using the configuration-interaction (CI) method, which includes the effects of direct (mean-field) Coulomb interaction among different charge carriers, exchange, and correlation. The entire method is described in detail elsewhere.<sup>22,27</sup> The CI method has been recently extended to include dipole-dipole Coulomb interaction<sup>28</sup> in order to describe exchange-splitting effects correctly.

The starting point of the simulation is an assumption on the QD structure. The present MBE growth conditions suggest a nonuniform In composition. Following Refs. 29–32 we assume a trumpet-shaped In composition. The vertical/lateral aspect ratio is expected to vary between QDs and is used as structural variation parameter.

The experimental data indicate that the symmetry of the investigated QDs is smaller than  $C_{2v}$ . The fine structure of the spectra depends on the structural symmetry. Therefore we consider deviations from structures with mathematically exact symmetry. This can be easily accounted for in atomistic models, such as the empirical pseudopotential<sup>33</sup> or the empirical tight-binding method.<sup>34,35</sup> In a mesoscopic model such as  $\mathbf{k}\cdot\mathbf{p}$ , in contrast, the virtual-crystal approximation (VCA), is typically used. In Ref. 22 we applied this approach to uniform and nonuniform composition profiles. By following this approach, the assumption of a symmetric structure leads to optical selection rules contrary to experimental observations.<sup>36</sup>

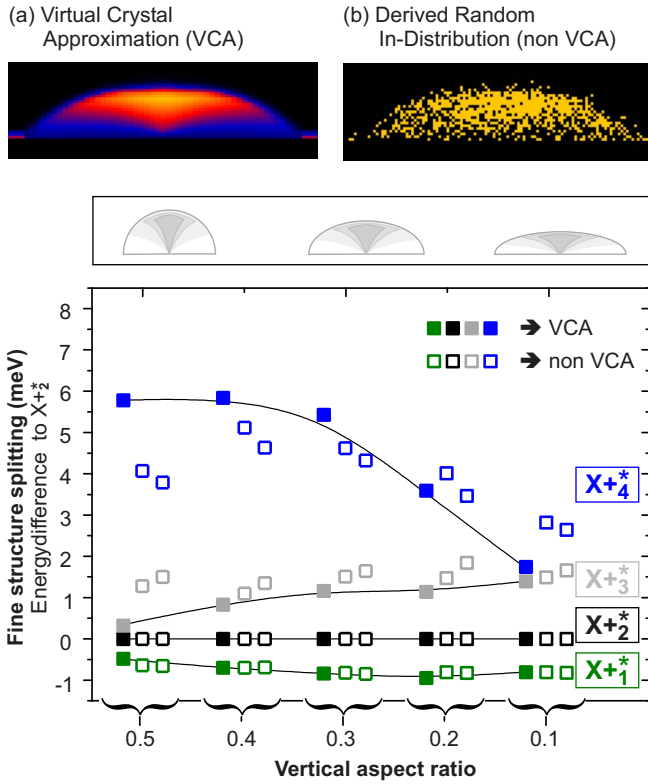


FIG. 4. (Color online) At the head: InGaAs distribution of (a) VCA and (b) non-VCA QDs. Lower panel: energies of hot trion states  $X_{+1,\dots,4}^*$  as a function of the vertical aspect ratio. Bold symbols refer to the VCA QDs open symbols to the non-VCA QDs.

To avoid this problem, we developed a “quasiatomic” or non-VCA description of QDs (Fig. 4). For a given fraction  $(x, 1-x)$  of  $\text{In}_x\text{Ga}_{1-x}\text{As}$  at a given grid point, InAs is chosen with probability  $x$  and GaAs with probability  $(1-x)$ . Since the choice is not unique, we applied this procedure twice for each QD, resulting in a series with twice as many structures as the series of VCA QDs.

Figure 4 shows the theoretical  $X_{+}^*$  fine structure of a series of QDs with varying aspect ratio and constant In amount. For each aspect ratio a VCA QD (full boxes) and two additional non-VCA QDs (open boxes) are calculated. From this plot three conclusions can be drawn. First, the predicted values for the fine-structure splitting of the  $X_{+}^*$  agree even quantitatively very well with the experimental data depicted in Fig. 3. This means that our approach reproduces also the relevant exciton fine structure correctly. Next, a variation in the aspect ratio of the QDs within a realistic range reproduces the anticorrelation between the  $X_{+4}^*-X_{+2}^*$  and the  $X_{+3}^*-X_{+2}^*$  splittings. Considering QDs with the same aspect ratio of 0.3, 0.4, or 0.5 the observed anticorrelation is also reproduced in each subseries. Hence the intermixing of the  $X_{+4}^*$  and  $X_{+3}^*$  states is determined by more than one structural parameter.

However, since the calculations are very complex and many effects are treated simultaneously, a mere agreement to experiment does not necessarily allow unambiguous conclusions. Therefore, we repeated the calculation for an example QD by omitting different parts of the model in the following steps (see Fig. 5).

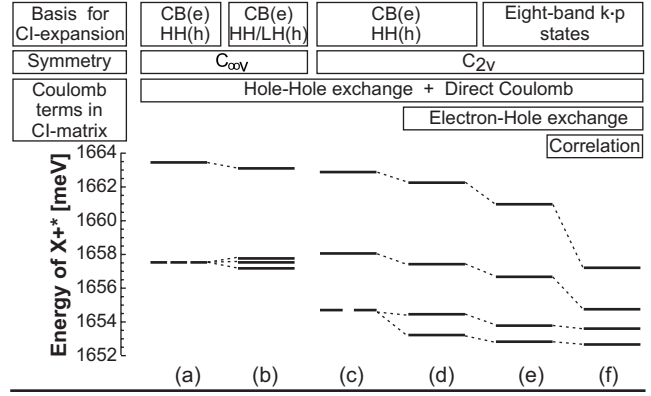


FIG. 5. Influence of specific parameters to the fine-structure splitting of the hot trion. The complexity in the model is increased from (a) to (f). Every single line represents a twofold (double line: fourfold; triple line: sixfold)-degenerate state.

(a) Isotropic hole-hole exchange: single-band projections of the eight-band  $\mathbf{k}\cdot\mathbf{p}$  orbitals are used as single-particle states (for simplicity we keep the original  $\mathbf{k}\cdot\mathbf{p}$  energies). They are calculated in the absence of a piezoelectric potential, hence, carry the  $C_{\infty 0}$  symmetry for the QD structure. Only hole-hole exchange terms are taken into account using a  $(2e, 4h)$  configuration. As a result, we obtain the singlet-triplet splitting of the  $X_{+1,\dots,4}^*$  states.

(b) Effects of light-hole contributions: in addition to (a) hole states are allowed to carry their original light-hole character (projection on heavy-hole and light-hole basis). As a consequence, the triplet state splits into three doublets. The triplet splitting is significantly smaller than the singlet-triplet splitting.

(c) Anisotropic hole-hole exchange: piezoelectricity is added, leading to a  $C_{2v}$ -confinement symmetry and laterally anisotropic wave functions.<sup>22</sup> Only heavy-hole projections are used for the hole states [similar to (a)]. The triplet state splits into a fourfold-degenerate state at lower energies and a twofold-degenerate state at higher energies caused by an intermixing between the singlet and one of the triplet states.

(d) Electron-hole exchange: in addition to (c) electron-hole exchange terms are accounted for. As a result the triplet state splits into three well-separated doubly-degenerate states.

(e) Eight-band  $\mathbf{k}\cdot\mathbf{p}$  basis states: the single-band projection basis is replaced by the original eight-band  $\mathbf{k}\cdot\mathbf{p}$  states. Thus the model accounts for intraband and interband mixings. The hole states now gain a small light-hole contributions of about 10%. The triplet states split into three twofold-degenerate states. The energies of the two energetically lowest triplet states and of the singlet state decrease significantly.

(f) Correlation: the many-body basis size is increased by using a  $(2e, 10h)$  configuration instead of  $(2e, 4h)$ . As a consequence, the energies of the two upper levels drop drastically by 3.7 and 2 meV, respectively. The two lower levels remain unaffected.

In this evolution effects of specific parts of the exchange and correlation become transparent. Quantitative predictions of the fine structure need to include correlation effects, as these affect the energy splittings strongly (f). In experiment

(Fig. 3) we observe an anticorrelation between the  $X_{+3}^* - X_{+2}^*$  and the  $X_{+4}^* - X_{+2}^*$  splittings, which can be explained by an intermixing of the  $X_{+3}^*$  and  $X_{+4}^*$  states. Theory reveals (c) that such intermixing can be caused only by the anisotropic part of the hole-hole exchange. This leads to an intermixing of the singlet state with one triplet state, causing an energy separation of this state to the remaining fourfold-degenerate triplet.

## V. CONCLUSION

Combination of  $\mu$ PL and  $\mu$ PLE spectra allows the unambiguous identification of sharp resonances in  $\mu$ PLE spectra detected on the  $X+$  luminescence as  $e_0-h_1$  excitations, resulting in the formation of a hot trion in the  $e_0h_0h_1$  configuration. The observation of such  $e_0-h_1$  transitions indicates a symmetry of the investigated QDs lower than  $C_{2v}$ . In PLE the complete fine structure of the hot trion is visible; the

absence of strict spin-selection rules for the hot trion states indicates intermixing of the triplet states. Detailed theory including anisotropic exchange and correlation reproduces the experimental data. The anisotropic hole-hole exchange interaction produces a mixing of the singlet with one triplet state.

The quantitative agreement between theory and experiment of the fine-structure splitting of the  $X+^*$  justifies the numerical method for calculating the exchange interaction. Therefore predictions of the fine structure of neutral excitons are now possible, being of largest importance for future electrically driven single qubit and entangled photon emitters.

## ACKNOWLEDGMENTS

We are indebted to A. E. Zhukov, G. E. Cirlin, and V. M. Ustinov for providing the samples. This work was partly funded by Sonderforschungsbereich 787 of DFG. The calculations were performed on an IBM p690 supercomputer at the HLRN Berlin/Hannover.

- 
- <sup>1</sup>O. Benson, C. Santori, M. Pelton, and Y. Yamamoto, Phys. Rev. Lett. **84**, 2513 (2000).
- <sup>2</sup>N. Akopian, N. H. Lindner, E. Poem, Y. Berlatzky, J. Avron, D. Gershoni, B. D. Gerardot, and P. M. Petroff, Phys. Rev. Lett. **96**, 130501 (2006).
- <sup>3</sup>R. M. Stevenson, R. J. Young, P. Atkinson, K. Cooper, D. A. Ritchie, and A. J. Shields, Nature (London) **439**, 179 (2006).
- <sup>4</sup>A. Lochmann, E. Stock, O. Schulz, F. Hopfer, D. Bimberg, V. Haisler, A. Toporov, A. Bakarov, and A. Kalagin, Electron. Lett. **42**, 774 (2006).
- <sup>5</sup>M. Scholz *et al.*, Opt. Express **15**, 9107 (2007).
- <sup>6</sup>R. Seguin, A. Schliwa, S. Rodt, K. Pötschke, U. W. Pohl, and D. Bimberg, Phys. Rev. Lett. **95**, 257402 (2005).
- <sup>7</sup>E. L. Ivchenko and G. E. Pikus, *Superlattices and Other Heterostructures*, Springer Series in Solid-State Sciences Vol. 110 (Springer, Berlin, 1997).
- <sup>8</sup>R. I. Dzhiyev, B. P. Zakharchenya, E. L. Ivchenko, V. L. Korenev, Y. G. Kusraev, N. N. Ledentsov, V. M. Ustinov, A. E. Zhukov, and A. F. Tsatsulnikov, Phys. Solid State **40**, 790 (1998).
- <sup>9</sup>T. Takagahara, Phys. Rev. B **62**, 16840 (2000).
- <sup>10</sup>M. Ediger, G. Bester, B. D. Gerardot, A. Badolato, P. M. Petroff, K. Karrai, A. Zunger, and R. J. Warburton, Phys. Rev. Lett. **98**, 036808 (2007).
- <sup>11</sup>B. Urbaszek, R. J. Warburton, K. Karrai, B. D. Gerardot, P. M. Petroff, and J. M. Garcia, Phys. Rev. Lett. **90**, 247403 (2003).
- <sup>12</sup>R. Seguin, S. Rodt, A. Schliwa, K. Pötschke, U. W. Pohl, and D. Bimberg, Phys. Status Solidi B **243**, 3937 (2006).
- <sup>13</sup>I. A. Akimov, K. V. Kavokin, A. Hundt, and F. Henneberger, Phys. Rev. B **71**, 075326 (2005).
- <sup>14</sup>R. Heitz, O. Stier, I. Mukhametzanov, A. Madhukar, and D. Bimberg, Phys. Rev. B **62**, 11017 (2000).
- <sup>15</sup>A. Zrenner, M. Markmann, A. Paassen, A. L. Efros, M. Bichler, W. Wegscheider, G. Böhm, and G. Abstreiter, Physica B **256-258**, 300 (1998).
- <sup>16</sup>Y. Toda, O. Moriwaki, M. Nishioka, and Y. Arakawa, Phys. Rev. Lett. **82**, 4114 (1999).
- <sup>17</sup>R. Oulton, J. J. Finley, A. I. Tartakovskii, D. J. Mowbray, M. S. Skolnick, M. Hopkinson, A. Vasanelli, R. Ferreira, and G. Bastard, Phys. Rev. B **68**, 235301 (2003).
- <sup>18</sup>M. E. Ware, E. A. Stinaff, D. Gammon, M. F. Doty, A. S. Bracker, D. Gershoni, V. L. Korenev, S. C. Badescu, Y. Lyanda-Geller, and T. L. Reinecke, Phys. Rev. Lett. **95**, 177403 (2005).
- <sup>19</sup>A. Vasanelli, R. Ferreira, and G. Bastard, Phys. Rev. Lett. **89**, 216804 (2002).
- <sup>20</sup>K. V. Kavokin, Phys. Status Solidi A **195**, 592 (2003).
- <sup>21</sup>S. Rodt, A. Schliwa, K. Pötschke, F. Guffarth, and D. Bimberg, Phys. Rev. B **71**, 155325 (2005).
- <sup>22</sup>A. Schliwa, M. Winkelkemper, and D. Bimberg, Phys. Rev. B **76**, 205324 (2007).
- <sup>23</sup>G. Bester, S. Nair, and A. Zunger, Phys. Rev. B **67**, 161306(R) (2003).
- <sup>24</sup>M. Grundmann, O. Stier, and D. Bimberg, Phys. Rev. B **52**, 11969 (1995).
- <sup>25</sup>G. Bester, X. Wu, D. Vanderbilt, and A. Zunger, Phys. Rev. Lett. **96**, 187602 (2006).
- <sup>26</sup>G. Bester, A. Zunger, X. Wu, and D. Vanderbilt, Phys. Rev. B **74**, 081305(R) (2006).
- <sup>27</sup>O. Stier, M. Grundmann, and D. Bimberg, Phys. Rev. B **59**, 5688 (1999).
- <sup>28</sup>A. Schliwa, R. Zimmermann, and D. Bimberg (unpublished).
- <sup>29</sup>N. Liu, J. Tersoff, O. Baklenov, A. L. Holmes, and C. K. Shih, Phys. Rev. Lett. **84**, 334 (2000).
- <sup>30</sup>T. Walthers, A. G. Cullis, D. J. Norris, and M. Hopkinson, Phys. Rev. Lett. **86**, 2381 (2001).
- <sup>31</sup>D. M. Bruls, J. W. A. M. Vugs, P. M. Koenraad, H. W. M. Salemink, J. H. Wolter, M. Hopkinson, M. S. Skolnick, F. Long, and S. P. A. Gill, Appl. Phys. Lett. **81**, 1708 (2002).
- <sup>32</sup>A. Lenz, R. Timm, H. Eisele, C. Hennig, S. K. Becker, R. L. Sellin, U. W. Pohl, D. Bimberg, and M. Dähne, Appl. Phys. Lett. **81**, 5150 (2002).
- <sup>33</sup>L. W. Wang, J. Kim, and A. Zunger, Phys. Rev. B **59**, 5678

(1999).

<sup>34</sup>R. Santoprete, B. Koiller, R. B. Capaz, P. Kratzer, Q. K. K. Liu, and M. Scheffler, Phys. Rev. B **68**, 235311 (2003).

<sup>35</sup>S. Lee, O. L. Lazarenkova, P. von Allmen, F. Oyafo, and G. Klimeck, Phys. Rev. B **70**, 125307 (2004).

<sup>36</sup>A. Schliwa and D. Bimberg (unpublished).